Aqueous Synthesis of Multi-Carbon Dots Crosslinked Polyethyleneimine Particles with Enhanced Photoluminescent Properties

Yuan Yao [a], Dechao Niu [a,b], Cheng Hao Lee [a], Yongsheng Li [b], and Pei Li [a] *

[a] Department of Applied Biology and Chemical Technology, The Hong Kong Polytechnic University, Hung Hom, Kowloon, Hong Kong, P. R. China

[b] School of Materials Science and Engineering, East China University of Science and Technology, Shanghai, P. R. China

Abstract

Fluorescent nanoparticles with high photostability, heavy-metal-free, and low toxicity are highly desirable as imaging probes for biological applications. Here, we report a novel synthetic strategy to prepare ultrabright multi-carbon dot crosslinked PEI particles, namely CDs@PEI, through self-assembly of hydrophobically modified PEI and *in situ* generations of carbon dots within residual monomer-swollen micelles. The resulting particles consist of numerous carbon dots, which are individually and homogeneously embedded within the PEI network and have an average hydrodynamic diameter of approximately 100 nm with ζ–potential above +35 mV. The CDs@PEI particles possess a synergistic effect of photoluminescent carbon dot and crosslink-enhanced emission of PEI, giving the particles with superior optical properties such as high fluorescence quantum yield (up to 66%) in the aqueous system, excitation-dependent emission phenomenon, stable fluorescence in a wide pH range, and resistance to photobleaching.

1. Introduction

In the past decade, the development of photo-stable, heavy-metal-free, and low toxicity photoluminescent nanoparticles for biological applications has attracted considerable attention.[1] Carbon dots (CDs) are promising fluorescent nanoparticles because of their convenient synthesis, strong fluorescence, high photostability, excellent biocompatibility, and low toxicity.[2] The carbon dots usually have sizes below 10 nm with surface functionality.[3] A convenient approach to achieving surface functionality is through surface passivation. The thin passivating layer on the carbon dot surface could significantly improve their photostability and quantum yield.[4] Branched polyethyleneimine (PEI) which consists of 25% primary, 50% secondary, and 25% tertiary amines has been used increasingly to transfect genes into living cells since its first report as a transfection agent in 1995.[5] Recently, PEI-passivated carbon dots (PEI-CD) have gained much interest in the biomedical field for molecular and pH sensing,[6] cellular imaging,[7] as well as gene and vaccine deliveries with bioimaging functions.[8-9] The PEI-CDs are fabricated through two main approaches: 1) PEI molecule acting as both the passivating agent and the carbon source is oxidized with either nitric acid at 120 ºC or with ammonium persulfate (APS) under hydrothermal treatment.[10-11] 2) PEI molecule acts as a passivating agent while a precursor molecule such as citric acid, glycerol, sucrose folic acid, hyaluronate (HA), or chitosan is used as a carbon source to generate carbon dots through either microwave radiation or hydrothermal treatment.[8-9,12-15] The quantum yields of the PEI-passivated carbon dots prepared by these methods are in the range of 2 to 54%. It is worth mentioning that all the current methods focus on the preparation of individually dispersed PEI-CD nanoparticles in aqueous systems with diameters less than 10 nm. Such ultrafine nanoparticles with the passivated layer can prevent carbon dots from fluorescent self-

quenching.[16-17] Furthermore, the nanosized carbon dots can be rapidly excreted from the animal body.[18] On the other hand, the PEI-based particles containing multiple carbon dots have not yet been exploited.

Recently, non-conjugated polymer dots with strong fluorescent emissions have been prepared through chemical crosslinking or physical immobilization of polymer chains.[19] The enhanced photoluminescent property of the polymer is attributed to the restriction of polymer chain movement through the chemical crosslinking of the polymer. This effect is named the crosslink-enhanced emission (CEE). Several studies have shown that crosslinking of polyethyleneimine using carbon tetrachloride,[20] aldehyde[21-23] or D-glucose[24] could generate PEI nanoparticles with strong fluorescence.

Herein, we report a novel synthetic strategy to prepare multi-carbon dots crosslinked PEI particles, namely CDs@PEI, through self-assembly of hydrophobically modified PEI, followed by *in situ* generations of carbon dots within residual monomer-swollen micelles. The resulting particles consist of numerous carbon dots, which are individually and homogeneously crosslinked with the PEI. Therefore, the CDs@PEI particles possess synergistic photoluminescent effects of carbon dot and crosslink-enhanced emission of PEI, giving the particles with superior optical properties such as high fluorescence quantum yield (up to 66%) in the aqueous system, excitation-dependent emission phenomenon, stable fluorescence in a wide pH range, and resistance to photobleaching. This new type of multiple carbon dot-crosslinked PEI particles represents a new design of carbon dot-based nanomaterials, which may find

potential application as an intrinsic photoluminescent nanocarrier for monitoring the drug and gene deliveries.

2. Results and Discussion

Scheme 1 illustrates the synthetic route to prepare the CDs@PEI particles. In the first stage, graft copolymerization of methyl methacrylate (MMA) from PEI was initiated with *t*-butyl hydroperoxide (TBHP) at 80 ^{o}C based on our previously established method.[25-26] The concentration of the TBHP used was equivalent to 10 mol% of the primary amine of the PEI to generate PEI-g-PMMA copolymer.[27- 28] When the grafted PMMA grew to the molecular weight to up to the appropriate hydrophobic/hydrophilic balance between the PEI and PMMA, the amphiphilic copolymer could undergo *in situ* self-assembly to form a micelle-like microdomain to minimize their surface energy. The polymerization was purposely stopped at 2 hours, giving approximately 50% monomer conversion as determined by the gravimetrical method and elemental analysis (Table S1). The actual composition of the resulting prepolymer contained 82.5% PEI and 17.5% PMMA based on the elemental analysis result. The preformed mixture appeared to be a slightly milky solution with a mean hydrodynamic diameter of 56.7 nm. Even though there was still around 50% monomer remaining in the solution, neither oil droplet nor phase-separated monomer layer was observed in the reaction mixture, indicating that the residual MMA molecules were swollen and stabilized within the preformed micelles. TEM image of the preformed particles showed that more than 90% of the dried nanoparticles were in the range of 8.3 to 23.9 nm (Figure S2). Moreover, most of these nanoparticles appeared as dark dots after staining with a diluted phosphotungstic acid solution, indicating that the nanoparticles mainly comprised the PEI component. Only a few larger amphiphilic

core-shell particles with diameters between 38 and 58 nm were present. These results suggest the formation of MMA swollen micelle nanoparticles in the first stage of graft polymerization.

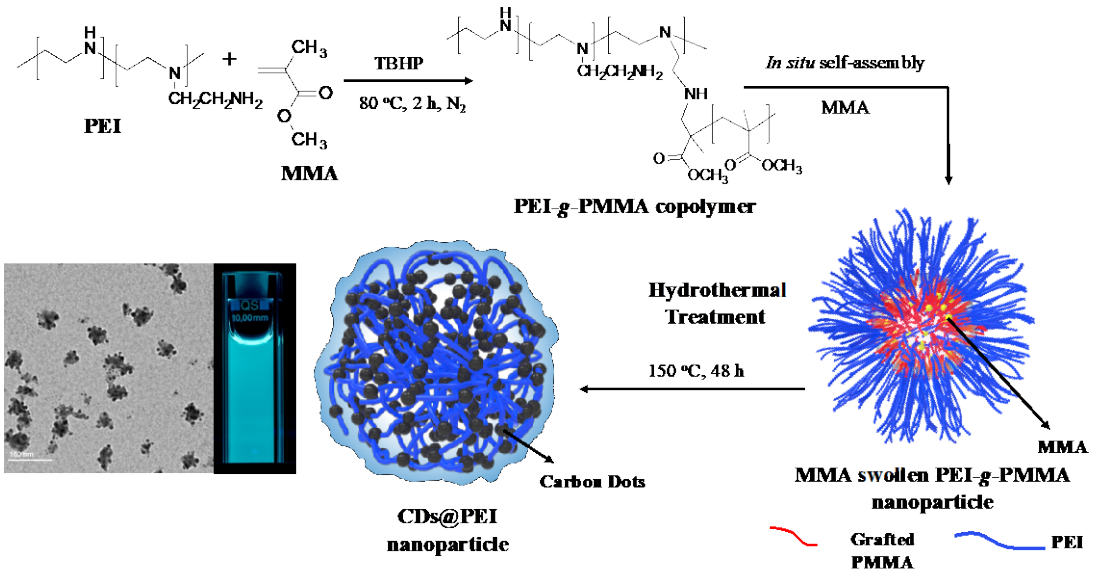

Scheme 1. Synthesis of CDs@PEI particles through a two-stage reaction: 1) The graft polymerization of MMA from PEI, followed by *in situ* self-assembly into MMA swollen PEI-*g*-PMMA micelle nanoparticle; 2) Hydrothermal treatment of the residual monomer-swollen micelles to generate the CDs@PEI particles.

In the second stage, the preformed MMA swollen nanoparticles were hydrothermally treated at 150 °C to generate carbon dots from the methyl methacrylate precursor (as the carbon source). Since the methoxy group of MMA molecule is a good leaving group, the amidation reaction between the PEI and MMA would easily occur during the hydrothermal process, resulting in crosslinking of the PEI with the carbon dots and generating multiple carbon dots crosslinked PEI network. In this system, the PEI molecule acted as a passivating agent to prevent individual carbon dots from aggregation. Thus, the resultant particles contained numerous carbon dots, which were

homogeneously distributed throughout the PEI network. Under the hydrothermal conditions, the preformed grafted PMMA was also converted into carbon dots via depolymerization of the PMMA to MMA monomer since the ceiling temperature of the PMMA is around 200 ºC at the atmospheric pressure.

To optimize the synthetic conditions, we have investigated the effect of thermal treatment time on the particle composition, diameter, morphology as well as size and crystallinity of the embedded carbon dots. Results of elemental analysis (Table S1) indicate that the carbon to nitrogen ratio increased with increasing thermal treatment time from 24 to 96 hours, suggesting that more and more carbon dots were generated with prolonged thermal treatment. Figure S1 shows the FTIR spectra of the native PEI, pure PMMA, preformed PEI-*g*-PMMA nanoparticles, and CDs@PEI particles obtained at thermal treatment times of 24, 48, and 96 hours. It was found that the characteristic peaks of PMMA (C=O stretching vibration at 1732 cm^{-1} and C-O-C stretching vibration at 1200 cm^{-1}) had reduced gradually, and eventually disappeared after 48 hours of thermal treatment. At the same time, the peak at 1650 cm^{-1} became broader, indicating the formation of amide bonding. Furthermore, the characteristic peaks of PEI (N-H stretching peak at 3420 cm^{-1}, bending vibrational peak at 1562 cm^{-1}, as well as C-N stretching vibrational peak at 1112 cm^{-1}) remained almost the same even after 96 hours of thermal treatment. These results suggest that the methyl methacrylate is the carbon source for the formation of carbon dots. The PEI molecule mainly serves as a passivating agent being crosslinked by the newly formed carbon dots, thus suppressing the C-dots from aggregation.

The particle sizes and distributions of the preformed PEI-*g*-PMMA and CDs@PEI obtained after thermal treatments of 24 hours (CDs@PEI-24), 48 hours (CDs@PEI-48) and 96 hours (CDs@PEI-96) were determined by the dynamic light scattering (DLS)

(Figure S3a). Results show that increasing thermal treatment time from 24 to 48 and 96 hours resulted in increasing average particle sizes from the initial 56.7 nm to 88.1, 99.5, and 106.9 nm, respectively. *zeta*-Potential values of the CDs@PEI particles as a function of pH from 3 to 10 were also investigated (Figure S3b). The preformed nanoparticles and all CDs@PEI particles possess positive surface charges with a similar trend under different solution pHs. The results suggest that these particles all contain PEI molecules on their particle surfaces. Finally, the dynamic movements of the CDs@PEI particles were detected by a Nanosight (Figure S4). Results show very stable and well-dispersed particles in water.

Morphology of the CDs@PEI particles and their stability in water was found to be strongly influenced by the thermal treatment time. After 24 hours of hydrothermal treatment, almost all the preformed MMA-swollen PEI-*g*-PMMA micelles and PEI/PMMA core-shell particles had disappeared (Figure S5). Instead, irregular particles containing plenty of carbon dots formed. After 48 hours of thermal treatment (CDs@PEI-48), the ill-defined CDs@PEI-24 particles became more spherical and compact. Prolonging the thermal treatment time to 96 hours (CDs@PEI-96) resulted in some degree of agglomeration of the resultant particles. Therefore, the optimal thermal treatment time was 48 hours, giving the highest quantum yield (Table S2).

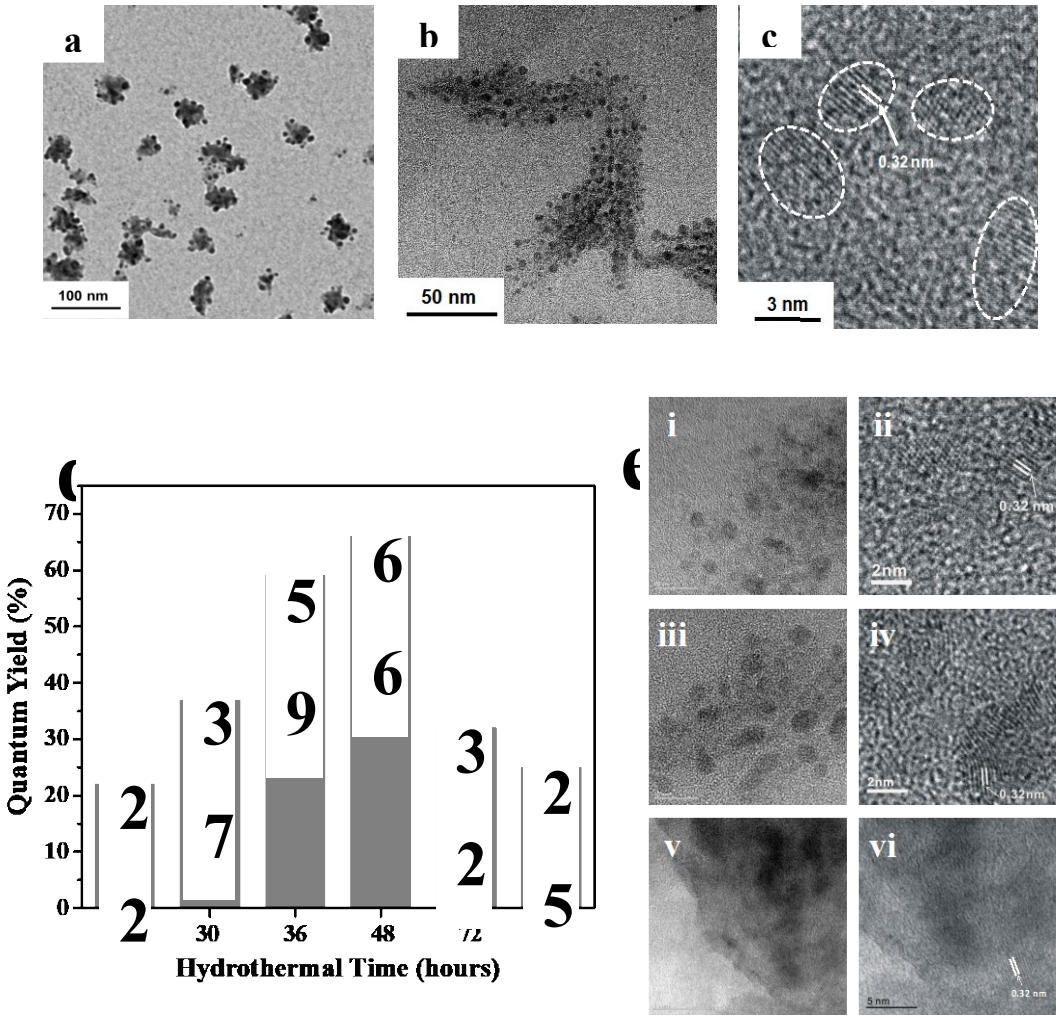

Figure 1. The morphologies of the CDs@PEI-48 particles and embedded carbon dots. a) TEM image of the CDs@PEI-48 particles stained with 0.5 w/w% phosphotungstic acid solution for 1 min. b) HRTEM image of CDs@PEI-48 particles without staining. c) High amplification of HRTEM image of embedded carbon dots having the lattice spacing of 0.32 nm. d) Effect of thermal treatment time on the absolute quantum yield of resultant CDs@PEI particles in water; e) HRTEM images of embedded carbon dots, their crystallinity, and lattice planes: CDs@PEI-24 (i, ii); CDs@PEI-48 (iii, iv); and CDs@PEI-96 (v, vi).

The morphology of the CDs@PEI-48 particles was further examined with the high-resolution transmission electron microscopy (HRTEM) without any staining treatment (Figure 1). The particles had an irregular shape and contained numerous carbon dots, which were homogeneously and individually distributed throughout the particle (Figures 1a and b). The carbon dots had diameters ranging from 3 to 6 nm (average diameter of 4.2 ± 0.7 nm) with a lattice spacing of 0.32 nm (Figure 1c). They acted as crosslinking sites to immobilize the PEI molecules, forming stable CDs@PEI particles in water. To verify the formation of carbon dots from the MMA precursors, a control experiment was conducted in which an aqueous mixture of branched PEI and MMA in a weight ratio of 2.5:1 was subjected to the hydrothermal treatment at 150 ^{o}C for 48 hours. Spherical carbon dots with diameters in the range of 2 to 6 nm (average diameter of 4.3 ± 0.6 nm) and lattice spacing of 0.32 nm were obtained (Figure. S6).

The fluorescence properties of the preformed PEI-*g*-PMMA nanoparticles and three CDs@PEI particles in water were investigated under UV radiation. Figure 2a shows that there is almost no fluorescence from the solution of the preformed PEI-*g*-PMMA nanoparticles under a 365 UV irradiation, while all other solutions of CDs@PEI particles display a bright blue color. Figure 2b presents the absorption spectra of both CDs@PEI particles and the control sample of single carbon dots. Both of them display strong absorption bands between 221 and 223 nm and moderate peaks at 367 nm. The results suggest that the fluorescence of both samples must have resulted from the nitrogen-doped surface states which involve the energy levels of functional groups between C n and C π*.[29] In fact, doping of carbon dots with a substituent containing nitrogen groups such as amide and amines has been reported to modulate the bandgap of the surface state of carbon dot, resulting in significantly enhancing fluorescence emission. [14, 30] Figure 2c exhibits the photoluminescent (PL) spectra of the CDs@PEI-

48 particles, which were irradiated with excitation wavelengths in the range of 300 to 480 nm. The strongest emission peak centered at 470 nm upon the excitation at 340 nm. We also found that the emission wavelength was not sensitive to the excitation wavelength in the excitation range of 300 to 360 nm. However, further increasing the excitation wavelengths from 380 to 480 nm shifted the emission peaks to longer wavelengths (520 nm) with reduced intensity. The normalized PL spectra shown in Figure 2d confirm the excitation-dependent emission property with excitation wavelengths above 380 nm. Moreover, the fluorescent lifetimes of three CDs@PEI samples (Figure S7) suggested that all samples had comparable short lifetime components ranging from 1.5 to 1.6 ns, and long lifetime components of 5.3 to 5.7 ns. The average fluorescent lifetimes of CDs@PEI nanoparticles were between 3.1 and 3.3 ns (Table S2). Such short lifetimes suggest the radiative recombination nature of excitations.[31-32]

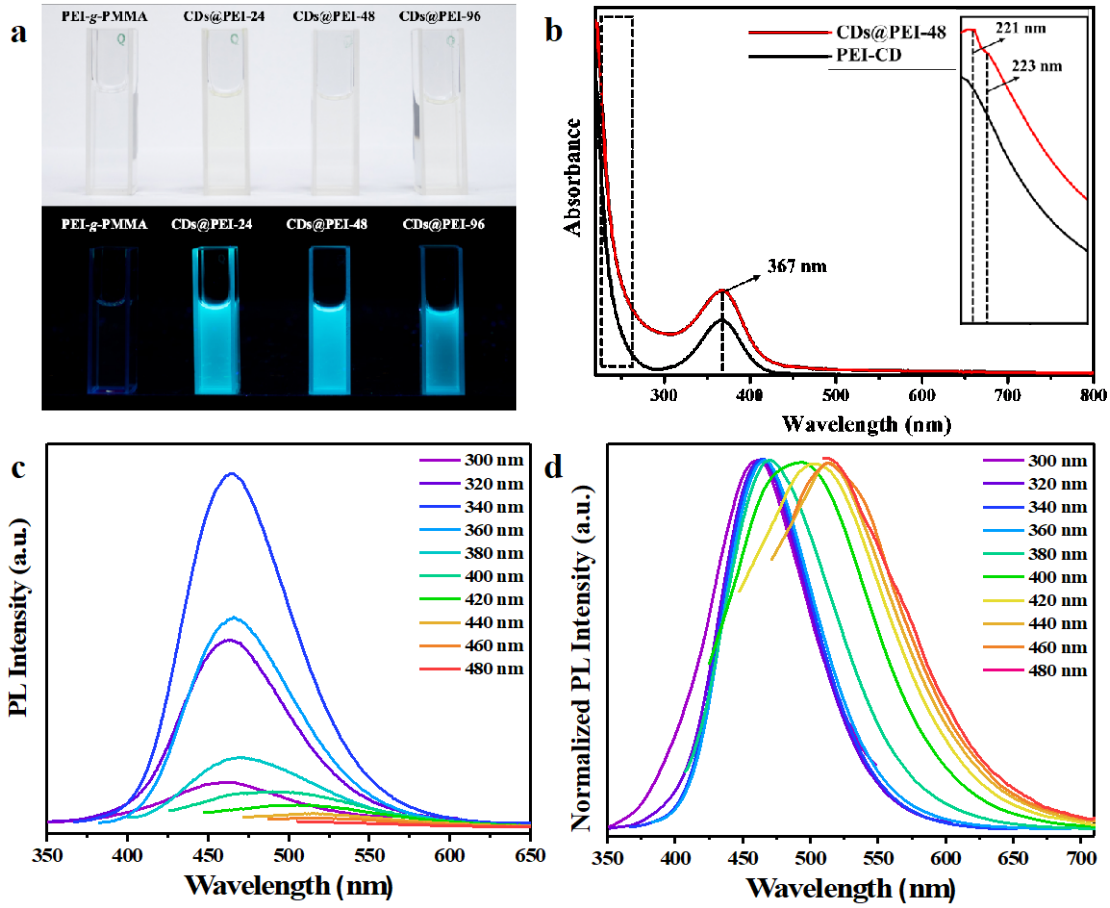

Figure 2. (a) Photos of PEI-*g*-PMMA nanoparticles and CDs@PEI particles under room light and 365 nm UV irradiation; (b) UV-Vis spectra of both CDs@PEI particles and control PEI-CD nanoparticles; (c) PL spectra of CDs@PEI-48 particles under different excitation wavelengths; (d) Normalized PL spectra of CDs@PEI-48 particles under different excitation wavelengths.

The effect of thermal treatment time on the absolute quantum yield (QY) of resultant CDs@PEI particles has been systematically studied. We found that increasing the thermal treatment time from 24, 30, 36 to 48 hours could enhance the QY from 22, 37, 59 to 66%, respectively. However, prolonging the hydrothermal time to 72 and 96 hours resulted in reducing the QY to 32% and 25%, respectively (Figure 1d). To understand this effect, we examined the morphology of CDs@PEI particles and the

crystallinities of carbon dots using a high-resolution transmission electron microscopy (HRTEM). Figure 1e(i) shows that after 24 hours of thermal treatment, individual carbon dots with a broad size distribution were formed in the PEI network. Their crystalline domains were ill-defined, indicating the formation of many defective and amorphous carbon dots at this stage [Figure 1e(ii)]. After 48 hours of thermal treatment, the carbon dots became more uniform and evenly distributed in the PEI network [Figure 1e(iii)], and formed a highly crystalline domain with a lattice spacing of 0.32 nm. Therefore, increasing the thermal treatment time to up to 48 hours could improve the size uniformity and crystallinity of the carbon dots, giving the highest quantum yield in the present work. When prolonging the hydrothermal treatment time to 96 hours, agglomeration of the carbon dots occurred as shown in Figure 1e(v) due to partial decomposition of the PEI molecule after extended thermal treatment. The aggregated CDs resulted in an aggregation-induced quenching, leading to a fluorescence turn-off phenomenon (Figure 1e (vi)).[33] These results suggest that complete surface passivation of individual carbon dots within the PEI network and high crystallinity of the carbon core are two critical factors for achieving high quantum yields of the CDs@PEI particles.

The absolute quantum yield of the CDs@PEI-48 particles was 66%, which is much higher than those of nitrogen-doped single carbon dot. Such high quantum yield may be attributed to the following three synergistic factors: 1) since the individually embedded carbon dots are fully covered by amine-rich PEI, the carbon dot surfaces have a homogeneous and high-density N-doped surface state, which can greatly enhance the fluorescence intensity;[31] 2) When individual carbon dots are dispersed in water, their electrons and holes generated from the surface state are easily quenched by

the surrounding environment such as water. In the case of CDs@PEI particles, the carbon dots are individually embedded within the PEI network. Thus, the electrons and holes generated from the CD surface states under irradiation are much easier to pair up with nearby carbon dots because they are within a few nanometers of one another. As a result, the quantum yield may enhance due to the effective radiative recombination process; 3) The PEI molecules are crosslinked with carbon dots, resulting in crosslink-enhanced emission (CEE). Based on all these results, we could conclude that the enhanced quantum yield of CDs@PEI particle over that of the singe PEI-CD nanoparticles is attributed to the synergistic effect of the high-density nitrogen-doping of carbon dots and the crosslink-enhanced emission property of the PEI.

Since the nitrogen-doped carbon dots could be considerably affected by the surrounding environment such as pH and irradiation,[34] the effects of solution pH and continuous excitation time on the fluorescence intensity of the CDs@PEI-48 particles were studied. Figure 3a shows that strong fluorescence intensities remain in a wide pH range (pH 1.2, 2.8, 4.7, 6.6, 8.4, and 10.3) under a 365 nm UV excitation. Furthermore, there were no apparent changes to the hydrodynamic sizes at different solution pH. Such excellent pH stability of the CDs@PEI particles may be attributed to two possible reasons: 1) Since all carbon dots are embedded within the PEI network, changing the solution pH mainly affect the PEI network, but has less influence on the surface state of the carbon dots; 2) The particle sizes of the CDs@PEI-48 particles at different solutions pHs were comparable, indicating that crosslinking of PEI molecules with carbon dots could retain the particle size under different pHs. Another important feature of the CDs@PEI-48 particles is their excellent photostability. The particles showed a small reduction in fluorescence intensity by only 8% after a continuous UV irradiation for 5 hours, while the single PEI-CD dots suffer from a significant decrease in

fluorescence (almost 50%) (Figure 3b). We believed that the superior photostability of CDs@PEI particles was attributed to the complete coverage of the carbon dots with the PEI network, thus protecting the surface molecules of the carbon dots from direct UV degradation.

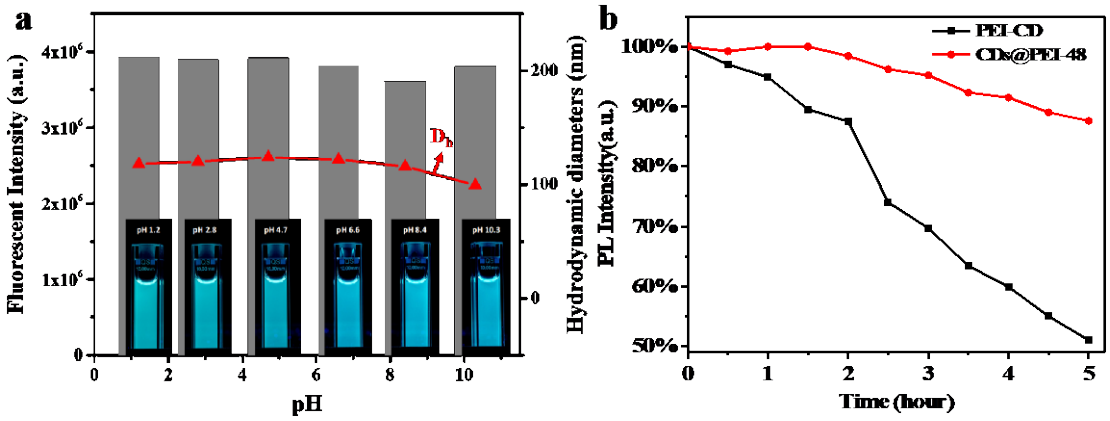

Figure 3. a) The PL intensity of CDs@PEI-48 particles at different solution pHs (from 1.2 to 10.3). b) PL intensities of CDs@PEI-48 and PEI-CD particles under a continuous UV irradiation for 5 hours.

3. Conclusions

We have successfully synthesized water-dispersible and ultrabright multi-carbon dots crosslinked polyethyleneimine particles through self-assembly of hydrophobically modified PEI and *in situ* generations of carbon dots within residual monomer-swollen micelles. This type of multi-carbon dot crosslinked PEI particles possess a synergistic photoluminescent effect of carbon dots and crosslinked PEI, giving high quantum yield (as high as 66%), multi-color emission, as well as pH- and photo-stable photoluminescence. We have evaluated the biological application of the CDs@PEI particles as intrinsic fluorescence nanocarriers including their *in vitro* and *in vivo* cytotoxicity, biodistribution, pharmacokinetic properties, and clearance from the

animal body using 4T1 tumor-bearing BALB/C mice as the animal model. Results will be published in a subsequent paper. The biological results demonstrate that the multi-carbon dot crosslinked PEI particles are promising intrinsic photoluminescent particles for imaging-guided diagnosis and therapy of cancer.

Supporting Information

Supporting Information is available from the Wiley Online Library or from the author.

Acknowledgment

This work was financially supported by the Hong Kong Polytechnic University, Hong Kong Research Grants Council General Research Fund (Project No. PolyU 153047/15P), and NSFC/RGC Joint Research Scheme (N_PolyU533/14). We also thank Prof. Jianhua Hao and Dr. Gongxun Bai for technical assistance with photoluminescent measurements.

Conflict of Interest

The authors declare no conflict of interest,

Keywords

Carbon dots, polyethyleneimine, crosslinking, fluorescence nanoparticle

References

[1] S. K. Bhunia, A. Saha, A. R. Maity, S. C. Ray, N. R. Jana, *Scientific Reports*, **2013**, *3*, 1473.

[2] J. Zhang, S. Yu, *Materials Today*, **2016**,*7*, 382

[3] K. Hola, Y. Zhang, Y. Wang, E. P. Giannelis, R. Zboril, A. L. Rogach, *Nano Today* **2014**, *9*, 590.

[4] Y. Park, J. Yoo, B. Lim, W. Kwon, S. W. Rhee, *J. Mater. Chem. A.* **2016**, *4*, 11582.

[5] O. Boussif, F. Lezoualc'h, M. A. Zanta, M. D. Mergny, D. Scherman, B. Demeneix, J. P. Behr, *Proc. Nat. Acad. Sci.* **1995**, *92*, 7297.

[6] H. Liu, R. S. Li, J. Zhou, C. Z. Huang, *Analyst*, **2017**, *142*, 4221.

[7] C. Wang, Z. Xu, C. Zhang, *ChemNanoMat,* **2015,** *1,* 122.

[8] C. Liu, P. Zhang, X. Zhai, F. Tian, W. Li, J. Yang, Y. Liu, H. Wang, W. Wang, W. Liu, *Biomaterials*, **2012**, *33*, 3604.

[9] S. Li, Z. Guo, G. Zeng, Y. Zhang, W. Xue, Z. Liu, *ACS Biomater. Sci. Eng.* **2018**, *4*,142.

[10] L. Shen, L. Zhang, M. Chen, X. Chen, J. Wang, *Carbon* **2013**, *55*, 343.

[11] L. Hu, Y. Sun, S. Li, X. Wang, K. Hu, L. Wang, X. Liang, Y. Wu, *Carbon* **2014**, *67*, 508.

[12] P. Pierrat, R. Wang, D. Kereselidze, M. Lux, P. Didier, A. Kichler, F. Pons, L. Lebeau, *Biomaterials* **2015**, *51*, 290.

[13] C. Ma, X. Zhang, L. Yang, Y. Wu, H. Liu, X. Zhang, Y. Wei, *Mater. Sci. Eng., C* **2016**, *68*, 37.

[14] M. Zhang, X. Zhao, Z. Fang, Y. Niu, J. Lou, Y. Wu, S. Zou, S. Xia, M. Sun, F. Du, *RSC Adv.* **2017**, *7*, 3369.

[15] L. Wang, Y. Yin, A. Jain, H. S. Zhou, *Langmuir* **2014**, *30*, 14270.

[16] Y. Song, S. Zhu, S. Xiang, X. Zhao, J. Zhang, H. Zhang, Y. Fu, B. Yang, *Nanoscale*, **2014**, *6*, 4676.

[17] Y. Chen, M. Zheng, Y. Xiao, H. Dong, H. Zhang, J. Zhuang, H. Hu, B. Lei, Y. Liu, *Adv. Mater.* **2016**, *28*, 312.

[18] M. Nurunnabi, Z. Khatun, K. M. Huh, S. Y. Park, D. Y. Lee, K. J. Cho, Y. Lee, *ACS Nano* **2013**, *7*, 6858.

[19] S. Zhu, Y. Song, J. Shao, X. Zhao, B. Yang, *Angew. Chem. Int. Ed.* **2015**, *54*, 14626.

[20] S. Zhu, L. Wang, N. Zhou, X. Zhao, Y Song, S. Maharjan, J. Zhang, L. Lu, H. Wang, B. Yang, *Chem. Commn.,* **2014**, *50*, 13845.

[21] S. G. Liu, N. Li, Y. Ling, B. H. Kang, S. Geng, N. B. Li, H. Q. Luo, *Langmuir*, **2016**, *32*, 1881.

[22] S. G. Liu, T. Liu, N. Li, S. Geng, J. L. Lei, N. B. Li, H. Q. Luo, *J. Phys. Chem. C.,* **2017**, *121*, 6874.

[23] Y. Ling, F. Qu, Q. Zhou, T. Li, Z. F. Gao, J. L. Lei, N. B. Li, H. Q. Luo, *Anal. Chem.*,**2015**, *87*, 8679.

[24] S. G. Liu, D. Luo, N. Li, W. Zhang, J. L. Lei, N. B. Li, H. Q. Luo, *ACS Appl. Mater. Interfaces,* **2016,** *8*, 21700.

[25] P. Li, J. Zhu, P. Sunintaboon, F. W. Harris, *Langmuir* **2002**, *18*, 8641.

[26] K. M. Ho, W. Y. Li, C. H. Lee, C. H. Yam, R. G. Gilbert, P. Li, *Polymer* **2010**, *51*, 3512.

[27] P. Sunintaboon, K. M. Ho, P. Li, S. Z. D. Cheng, F. W. Harris, *J. Am. Chem. Soc.* **2006**, *128*, 2168.

[28] C. H. Lee, C. H. Wong, D. Ouhab, R. Borsali, P. Li, *Langmuir* **2013**, *29*, 7583.

[29] J. Gu, M. J. Hu, Q. Q. Guo, Z. F. Ding, X. L. Sun, J. Yang, *RSC Adv.* **2014**, *4*, 50141.

[30] Y. Sun, B. Zhou, Y. Lin, W. Wang, K. A. S. Fernando, P. Pathak, M. J. Meziani, B. A. Harruff, X.Wang, H. Wang, P. G. Luo, H. Yang, M. E. Kose, B. Chen, L. M. Veca, S Xie, *J. Am. Chem. Soc.* **2006**, 128, 7756.

[31] Y. Dong, H. Pang, H. B. Yang, C. Guo, J. Shao, Y. Chi, C. M. Li, T. Yu, *Angew. Chem.* **2013**, *52,* 7800.

[32] H. Zhu, X. Wang, Y. Li, Z. Wang, F. Yang, X. Yang, *Chem. Commun.* **2009**, 5118.

[33] S. Hill, M. C. Galan, *Beilstein J. Org. Chem.* **2017**, *13*, 675.

[34] S. Zhu, Q. Meng, L. Wang, J. Zhang, Y. Song, H. Jin, K. Zhang, H. Sun, H. Wang, B. Yang, *Angew. Chem.* **2013**, *52*, 3953.